


# Visualization of Inter- and Intramolecular Interactions in Poly(3-hydroxybutyrate)/Poly(L-lactic acid) (PHB/PLLA) Blends During Isothermal Melt Crystallization Using Attenuated Total Reflection Fourier Transform infrared (ATR FT-IR) Spectroscopic Imaging

Applied Spectroscopy  
2021, Vol. 75(8) 980–987  
© The Author(s) 2021



Article reuse guidelines:  
sagepub.com/journals-permissions  
DOI: 10.1177/00037028211010216  
journals.sagepub.com/home/asp



Huiqiang Lu<sup>1</sup>, Harumi Sato<sup>2</sup>, and Sergei G. Kazarian<sup>1</sup> 

## Abstract

Inter- and intramolecular interactions in multicomponent polymer systems influence their physical and chemical properties significantly and thus have implications on their synthesis and processing. In the present study, chemical images were obtained by plotting the peak position of a spectral band from the data sets generated using in situ attenuated total reflection Fourier transform infrared (ATR FT-IR) spectroscopic imaging. This approach was successfully used to visualize changes in intra- and intermolecular interactions in poly(3-hydroxybutyrate)/poly(L-lactic acid) (PHB/PLLA) blends during the isothermal melt crystallization. The peak position of  $\nu(\text{C}=\text{O})$  band, which reflects the nature of the intermolecular interaction, shows that the intermolecular interactions between PHB and PLLA in the miscible state ( $1733\text{ cm}^{-1}$ ) changes to the inter- and intramolecular interaction ( $\text{CH}_3\cdots\text{O}=\text{C}$ ,  $1720\text{ cm}^{-1}$ ) within PHB crystal during the isothermal melt crystallization. Compared with spectroscopic images obtained by plotting the distribution of absorbance of spectral bands, which reveals the spatial distribution of blend components, the approach of plotting the peak position of a spectral band reflects the spatial distribution of different intra- and intermolecular interactions. With the process of isothermal melt-crystallization, the disappearance of the intermolecular interaction between PHB and PLLA and the appearance of the inter- and intramolecular interactions within the PHB crystal were both visualized through the images based on the observation of the band position. This work shows the potential of using in-situ ATR FT-IR spectroscopic imaging to visualize different types of inter- or intramolecular interactions between polymer molecules or between polymer and other additives in various types of multicomponent polymer systems.

## Keywords

Attenuated total reflection Fourier transform infrared, ATR FT-IR spectroscopic imaging, image, phase separation, biopolymer blend, poly(3-hydroxybutyrate), poly(L-lactide), FT-IR spectroscopy

Date received: 18 February 2021; accepted: 22 March 2021

## Introduction

Poly(3-hydroxybutyrate) (PHB) is one of the most popular biodegradable polymers derived from microorganisms. It is a semi-crystalline polyester with a glass transition temperature ( $T_g$ ) of approximately  $4^\circ\text{C}$ .<sup>1–4</sup> Poly(L-lactic acid) (PLLA) is also a biodegradable semi-crystalline polyester derived from chemical synthesis.<sup>5,6</sup> PLLA is one of the most widely used biodegradable polymers. The melting points of high molecular weight PHB and PLLA are similar,

<sup>1</sup>Department of Chemical Engineering, Imperial College London, South Kensington Campus, London, UK

<sup>2</sup>Graduate School of Human Development and Environment, Kobe University, Kobe, Japan

### Corresponding authors:

Harumi Sato, Kobe University, Tsurukabuto 3-11 Nada, Kobe 657-8501, Japan.

Email: hsato@tiger.kobe-u.ac.jp

Sergei G. Kazarian, Imperial College London, South Kensington Campus, London SW7 2AZ, UK.

Email: s.kazarian@imperial.ac.uk

170–180 °C. PHB has a high crystallinity of approximately 60–70% from the perfect stereo regularity produced by bacteria, while PLLA has a lower crystallinity due to its slower crystallization rate. PHB has an intermolecular hydrogen bond between the O atom of C=O group and the H atom of CH<sub>3</sub> group that links two adjacent parallel chains in the crystal lamellae.<sup>7–19</sup> Although the CH<sub>3</sub>···O=C hydrogen bonding in PHB is weak, this hydrogen bond has been found to play an important role in chain folding and stabilization of the crystal lamellae.<sup>7–19</sup> It can also enhance the ‘molecular friction’ in the polymer molecular chain, which affects polymer process largely.

The PHB/PLLA blend shows biodegradability and good compatibility. Their properties can be controlled by the ratio of blend components, which may lead to the expansion of applications for biodegradable polymers. It has been reported that PHB/PLLA blends with high molecular weight blend components are immiscible in the molten state, while blends of PHB with a low-molecular-weight PLLA ( $M_w < 18\,000$ ) are miscible in the molten state.<sup>20–23</sup> Since both PHB and PLLA are semi-crystalline polymers, these polymer blends crystallize at temperatures below their melting points. The PHB ( $M_w = 5000$ )/PLLA ( $M_w = 50\,000$ ) blend shows upper critical solution temperature (UCST) curves in the available temperature range.<sup>24</sup> In our previous study, simultaneous visualization of phase separation and crystallization in PHB/PLLA blends was realized using in situ attenuated total reflection (ATR) Fourier transform infrared (FT-IR) spectroscopic imaging. The appearance and gradual separation of crystalline polymer-rich domains were clearly shown in the time-dependent ATR FT-IR spectroscopic images.<sup>24</sup> These ATR FT-IR spectroscopic images were prepared using integrated absorbance of the  $\nu(\text{C}=\text{O})$  band of crystalline PHB (1730–1700  $\text{cm}^{-1}$ ) and the  $\nu(\text{C}=\text{O})$  band of crystalline PLLA (1762–1753  $\text{cm}^{-1}$ ).

In the PHB/PLLA blend system, crystallization and phase separation occur simultaneously because both blend components are crystallizable polymers.<sup>20,24</sup> An important finding in our imaging study was that as the phase separation progresses, the intermolecular interactions between PHB and PLLA in the miscible state change to inter- and intramolecular hydrogen bonds between PHBs in the immiscible state. Since the situation of inter- and intramolecular hydrogen bonds can be reflected by the position of the  $\nu(\text{C}=\text{O})$  band in the spectrum, the change of intermolecular interactions results in a unique peak shift of the  $\nu(\text{C}=\text{O})$  band that cannot be observed in the immiscible PHB/PLLA blend and PHB homopolymer.<sup>20</sup> Therefore, the aim of the present study is to visualize the change in intra- and intermolecular interactions induced by both phase separation and crystallization using ATR FT-IR spectroscopic images obtained on the position of spectral band. This methodology was first reported by Kazarian et al. in the observation of the crystalline polymorphs of drugs.<sup>25</sup> Then, Shinzawa et al. reported that NIR imaging analysis by band position shift was useful in the tablet analysis containing cellulose.<sup>26,27</sup> In the present

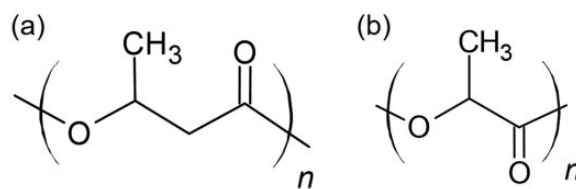


**Figure 1.** Chemical structures of (a) PHB and (b) PLLA.

study, we attempted to use ATR FT-IR spectroscopic imaging based on the observation of the band position to analyze inter- and intramolecular interactions in polymer blends. Moreover, through comparing the obtained images based on the observation of the band position with images obtained by plotting the distribution of integrated absorbance,<sup>28–34</sup> we have demonstrated the potential of the analysis of the images, produced by in-situ ATR FT-IR spectroscopic imaging, based on the band position as a new approach to visualize different types of inter- or intramolecular interactions. To the best of our knowledge, this is the first study to visualize different types of inter- or intramolecular interactions between polymer molecules in the multicomponent polymer system through spectroscopic images based on the position of spectral bands.

## Experimental

### Samples

The PHB ( $M_w = 5000$  g/mol, Fig. 1a) was obtained from Polysciences, Inc., and PLLA ( $M_w = 50\,000$  g/mol, Fig. 1b) was purchased from BMG Inc., Japan. The melting temperatures ( $T_m$ ) of PHB ( $M_w = 5000$  g/mol) and PLLA ( $M_w = 50\,000$  g/mol) are 163 and 182 °C, respectively.

### Preparation of the PHB/PLLA Blend

The PHB and PLLA were dissolved in chloroform with a weight ratio (PHB/PLLA = 75/25). The polymer blend solution was then stirred (300 rpm) at room temperature even after both PHB and PLLA were completely dissolved to prevent phase separation prior to the ATR FT-IR measurements. During the measurement, the polymer blend solution was cast on the measuring surface of the ATR crystal forming a thin film covering the whole diamond. An ATR FT-IR spectrometer was used to monitor whether the chloroform remaining in the sample had completely evaporated. The process of isothermal melt crystallization is the same as that in our previous research.<sup>24</sup>

### Macro ATR FT-IR Spectroscopic Imaging Measurement

A focal plane array (FPA) detector (Santa Barbara Focalplane), connected with a Tensor 27 FT-IR

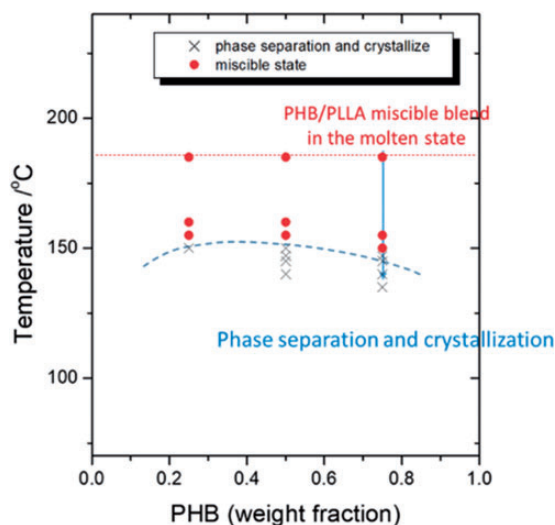
spectrometer (Bruker Corp.), was used to measure ATR FT-IR images in continuous scan mode. Spectra were collected with a  $4\text{ cm}^{-1}$  spectral resolution and 64 scans in the range of  $3900\text{--}850\text{ cm}^{-1}$ . The FPA detector has 4096 small pixels arranged in a  $64 \times 64$  grid format. Each pixel measures an infrared spectrum, and 4096 spectra are acquired in a single measurement. A diamond ATR accessory (Golden Gate, Specac Ltd.) aligned in the IMAC large sample compartment attached to the FT-IR spectrometer. The obtained data were recorded with Opus (Bruker Corp.) and analyzed using Matlab. According to the Beer–Lambert Law, the absorbance of a spectral band is proportional to the concentration of its corresponding component. Thus, through plotting the integrated absorbance of a certain band as colors, the concentration and spatial distribution of each component can be obtained.<sup>23,24</sup> In terms of spectroscopic images based on the observation of the band position,<sup>25–27</sup> the wavenumber of maximum absorbance in the  $\nu(\text{C}=\text{O})$  band region of PHB and PLLA for all of the pixels were obtained through Matlab. Spectroscopic images based on the observation of the band position were produced using GraphR to reveal the distribution of peak positions. A color bar from red (high value) to blue (low value) is attached beside the obtained images. The imaging area is approximately  $0.6 \times 0.55\text{ mm}^2$  with a spatial resolution of approximately  $10\text{--}12\text{ }\mu\text{m}$ . The size of PHB spherulites may range from ten to hundreds of micrometers depending on conditions and molecular weights.<sup>35,36</sup>

## Results and Discussion

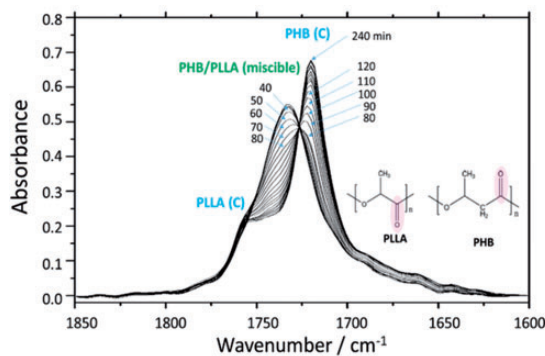
### Phase Separation and Crystallization Processes of PHB/PLLA (75/25) Blend Monitored Using ATR FT-IR Images Based on the Band Position

Figure 2 shows the phase diagram of PHB/PLLA blends ( $M_{w,\text{PHB}} = 5000$  and  $M_{w,\text{PLLA}} = 50\,000$ ), which indicates the critical temperature for phase separation and crystallization at different compositions. In the present study, the PHB/PLLA (75/25) blend with a higher concentration of PHB was selected as the sample, because the  $\nu(\text{C}=\text{O})$  band of crystalline PHB is more independent than that of crystalline PLLA, as shown in Figure S1 (Supplemental Material). In the PHB/PLLA (75/25) blend, phase separation and crystallization have been found to occur less than or equal to  $145\text{ }^\circ\text{C}$ .<sup>24</sup>

Figure 3 shows the time-dependent ATR FT-IR spectra in the  $\nu(\text{C}=\text{O})$  band region of PHB/PLLA (75/25) blend during phase separation and crystallization at  $145\text{ }^\circ\text{C}$ . At least three bands at  $1720$ ,  $1733$ , and  $1756\text{ cm}^{-1}$  appear in the  $\nu(\text{C}=\text{O})$  band region. These bands are assigned to  $\text{C}=\text{O}$  stretching modes of the crystalline PHB (PHB(C)), miscible PHB/PLLA blend, and crystalline PLLA (PLLA(C)), respectively. For the PHB/PLLA (75/25) blend, the absorbance of  $\nu(\text{C}=\text{O})$  band of crystalline PLLA should be low because of



**Figure 2.** The phase diagram of PHB/PLLA blends ( $M_{w,\text{PHB}} = 5000$  and  $M_{w,\text{PLLA}} = 50\,000$ ). Reproduced from Lu et al.<sup>24</sup> with permission of the American Chemical Society.



**Figure 3.** Time-dependent ATR FT-IR spectra of PHB/PLLA (75/25) blend during phase separation and crystallization at  $145\text{ }^\circ\text{C}$ . The  $\nu(\text{C}=\text{O})$  bands of crystalline PHB (PHB(C)), miscible state of PHB/PLLA blend, and crystalline PLLA (PLLA(C)) are  $1720$ ,  $1733$ , and  $1756\text{ cm}^{-1}$ , respectively.

its low concentration and degree of crystallization. Therefore, the research focus in the phase separation and crystallization process of PHB/PLLA (75/25) blends is the  $\nu(\text{C}=\text{O})$  band of crystalline PHB. During the isothermal crystallization process, the  $\nu(\text{C}=\text{O})$  band at  $1733\text{ cm}^{-1}$  ascribed to the miscible state of PHB/PLLA blend decreases and shifts gradually as a function of time, and finally it moves to  $1720\text{ cm}^{-1}$  as the  $\nu(\text{C}=\text{O})$  band of crystalline PHB. Therefore, the occurrence of band position shift may indicate the changes of the status of  $\nu(\text{C}=\text{O})$  band during phase separation and crystallization process of PHB/PLLA (75/25) blend at  $145\text{ }^\circ\text{C}$  as a function of time.

In our previous study, the peak position of  $\nu(\text{C}=\text{O})$  band did not show a shift during isothermal crystallization process of pure PHB.<sup>20</sup> However, a peak position shift occurs

in the  $\nu(\text{C}=\text{O})$  band during isothermal crystallization process of PHB/PLLA blends.<sup>24</sup> It indicates that the intermolecular interaction between PHB and PLLA in the miscible state is transformed into the inter- and intramolecular interaction within PHB crystal in the immiscible state.<sup>24</sup> Therefore, this study laid the basis for the use of ATR FT-IR spectroscopic images based on the observation of the band position as an efficient method to visualize the changes in these inter- and intramolecular interactions during the phase separation and crystallization of PHB/PLLA blends.

Figure S2 (Supplemental Material) plots the peak position of the  $\nu(\text{C}=\text{O})$  band versus time of isothermal crystallization at 145 °C in PHB/PLLA (75/25) blends. It can be observed from Fig. S2 that there is no shift in the peak position after 120 min, while the absorbance increase continues. The  $\nu(\text{C}=\text{O})$  band of crystalline PLLA was also shown clearly at 1756  $\text{cm}^{-1}$  in the spectra; however, it is difficult to analyze the peak shift from the miscible state to PLLA crystalline state because its absorbance is too low as shown in Fig. 3. Therefore, the analysis of the images based on the observation of the band position mainly depends on the  $\nu(\text{C}=\text{O})$  band of the miscible state and PHB's crystalline state. The  $\nu(\text{C}=\text{O})$  band at 1733  $\text{cm}^{-1}$  represents the intermolecular interaction between PHB and PLLA in the miscible state while the  $\nu(\text{C}=\text{O})$  band at 1720  $\text{cm}^{-1}$  represents the inter- and intramolecular interactions within the PHB crystal.

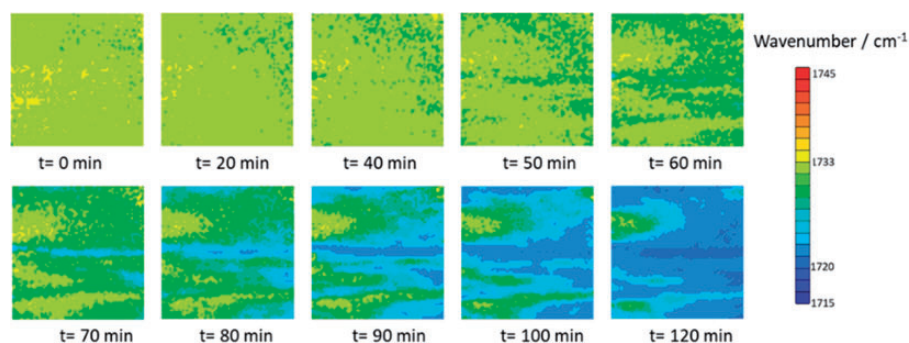
### Spectroscopic Images Based on the Observation of the Band Position of the PHB/PLLA (75/25) Blend

Figure 4 depicts time-dependent ATR FT-IR images based on the observation of  $\nu(\text{C}=\text{O})$  band position in the PHB/PLLA (75/25) blend at 145 °C, which shows time-dependent peak position shift of  $\nu(\text{C}=\text{O})$  band in each pixel. The wavenumber range of all images is the same (maximum (red) is 1745  $\text{cm}^{-1}$ , minimum (blue) is 1715  $\text{cm}^{-1}$ ). The obtained spectroscopic images clearly show the spatial distribution of the peak position of the  $\nu(\text{C}=\text{O})$  band.

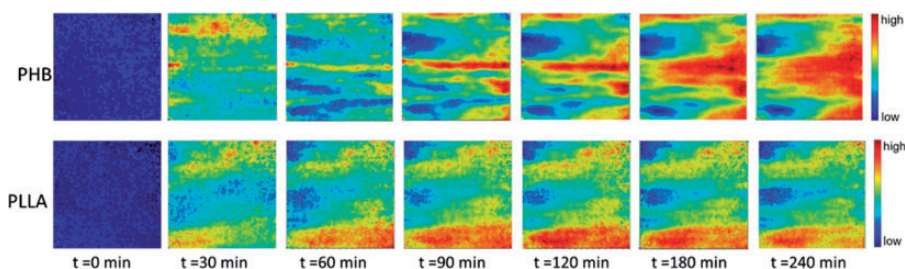
The peak position is defined by “the wavenumber of the band with the greatest absorbance”. Soon after reaching the isothermal crystallization temperature, the peak position of almost all pixels stays at 1733  $\text{cm}^{-1}$ , which indicates that the intermolecular interaction between PHB and PLLA appears in the whole polymer blend. After 1 h, the peak position of the pixels in the right part of image becomes less than 1733  $\text{cm}^{-1}$ , which means that the intermolecular interaction between PHB and PLLA has broken. With increasing annealing time from 60 to 120 min, the intermolecular interaction between PHB and PLLA, which is indicated by yellow and yellow green, disappears gradually in the images. On the other hand, the inter- and intramolecular interaction within PHB crystal, which is indicated by blue, start to occur in a larger area.

Figure 5 displays the images obtained by plotting the distribution of absorbance of spectral bands of PHB/PLLA (75/25) blend during the isothermal crystallization process at 145 °C. It can be clearly found that PHB and PLLA are miscible in the blend soon after decreasing to 145 °C, which agrees well with the corresponding images based on the observation of the band position: the intermolecular interaction between PHB and PLLA appears in the whole polymer blend. After 2 h, it can be seen that phase separation occurs, which is consistent with the disappearance of intermolecular interaction between PHB and PLLA shown in the corresponding images based on the observation of the band position. In addition, crystalline PHB-rich domains (Fig. 5; (120 min)) are located in the same place as the inter- and intramolecular interactions within PHB crystal occur, as shown in Fig. 4 (120 min). These results indicate that the images based on the observation of the band position are in good agreement with the images obtained by plotting the distribution of integrated absorbance.

Figure 6 presents the time-dependent absorbance change of the band assigned to the miscible state of PHB/PLLA blend and crystalline PHB, the peak position of  $\nu(\text{C}=\text{O})$  band of PHB crystal, and the second derivatives intensity of  $\nu(\text{C}=\text{O})$  band of PLLA crystal. The peak of



**Figure 4.** Spectroscopic images of the PHB/PLLA (75/25) blend generated by plotting the peak position (from 1745 to 1715  $\text{cm}^{-1}$ ) of the  $\nu(\text{C}=\text{O})$  band during isothermal crystallization process at 145 °C as a function of time. The size of each image is 0.6 mm  $\times$  0.55 mm.



**Figure 5.** Spectroscopic images of the PHB/PLLA (75/25) blend as a function of time during the isothermal crystallization process at 145 °C. The images were prepared based on the distribution of integrated absorbance of the  $\nu(\text{C}=\text{O})$  band of PHB crystal (1730–1700  $\text{cm}^{-1}$ , top) and that of PLLA crystal (1762–1753  $\text{cm}^{-1}$ , bottom). The size of each image is 0.6 mm  $\times$  0.55 mm.

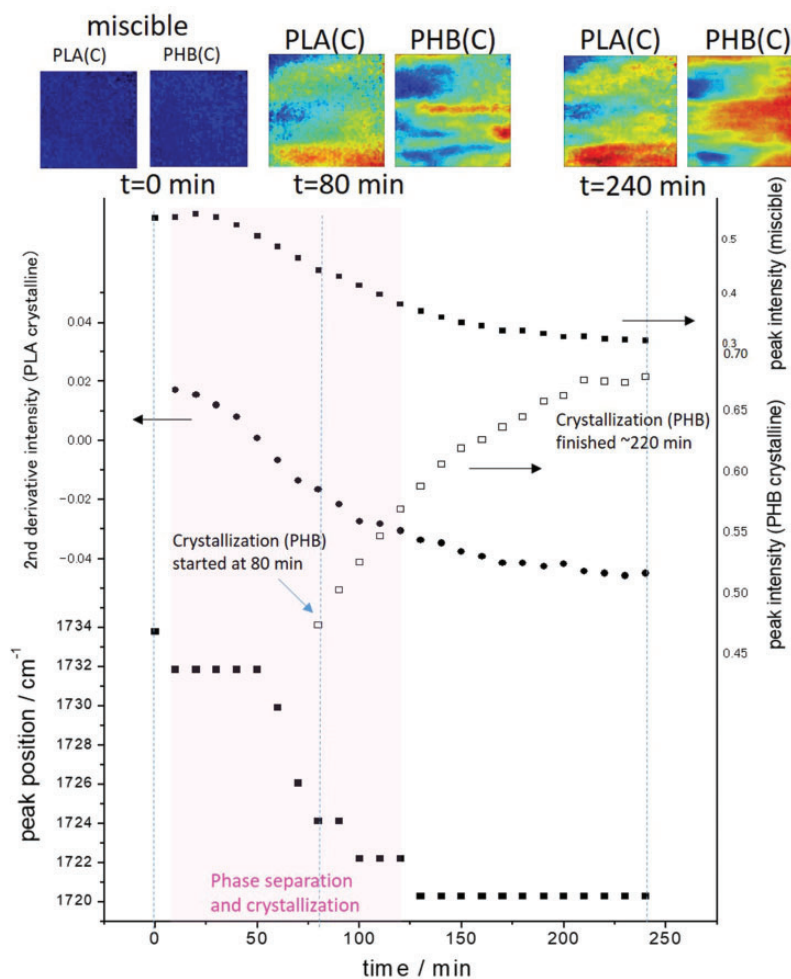


**Figure 6.** Time-dependent absorbance change of the  $\nu(\text{C}=\text{O})$  band assigned to the miscible state of the PHB/PLLA blend and crystalline PHB, second derivatives intensity of  $\nu(\text{C}=\text{O})$  band of PLLA crystal, and peak position of  $\nu(\text{C}=\text{O})$  band of PHB crystal with spectroscopic images based on the integrated absorbance of the  $\nu(\text{C}=\text{O})$  band of PHB crystal at 1730–1700  $\text{cm}^{-1}$  region (PHB(C)) and that of PLLA crystal at 1762–1753  $\text{cm}^{-1}$  region (PLLA(C)) during the isothermal crystallization process at 145 °C. The size of each image is 0.6 mm  $\times$  0.55 mm.

$\nu(\text{C}=\text{O})$  band of PLLA crystal at 1756  $\text{cm}^{-1}$  is clear but weak because of the low concentration of PLLA. Therefore, the second-derivative intensity of  $\nu(\text{C}=\text{O})$  band of PLLA crystal at 1756  $\text{cm}^{-1}$  is plotted in Fig. 6.

As shown in Fig. 6 after the temperature reaches 145 °C, the absorbance of the band at 1733  $\text{cm}^{-1}$ , which represents the miscible state of PHB/PLLA blend, decreases gradually. Meanwhile, the  $\nu(\text{C}=\text{O})$  band of PLLA crystal appears and

the  $\nu(\text{C}=\text{O})$  band of miscible state of PHB/PLLA blend starts to shift to  $1720\text{ cm}^{-1}$ . After around 80 min, the absorbance of  $\nu(\text{C}=\text{O})$  band of PHB crystal at  $1720\text{ cm}^{-1}$  starts increasing. Since the concentration of PLLA in the PHB/PLLA (75/25) blend is low,  $\nu(\text{C}=\text{O})$  band of PLLA crystal appears as a shoulder peak. And the absorbance of  $\nu(\text{C}=\text{O})$  band of PHB crystal starts increasing when the peak shift almost finishes. In this system, the molecular weight of PLLA is larger than that of PHB. Furthermore, PLLA crystallization temperature ( $\sim 160^\circ\text{C}$ ) is also higher than that of PHB ( $\sim 150^\circ\text{C}$ ). Therefore, in the phase separation and crystallization process of PHB/PLLA (75/25) blend at  $145^\circ\text{C}$ , PLLA crystals appear first.

### Comparison Between the Images Obtained by Distribution of the Position of the Band and by the Distribution of Absorbance of the Same Spectral Band

Here, the peak images are compared based on the observation of the band position with images obtained by plotting the distribution of integrated absorbance. As mentioned in the section above, both spectroscopic images based on the observation of the position of the band and integrated of the absorbance of the band show a good correspondence during the isothermal crystallization process. Fig. S3 presents the time-dependent spectroscopic images based on the observation of the band position (Fig. S3a) and images based on the distribution of integrated absorbance (Figs. S3b and S3c) in the  $\nu(\text{C}=\text{O})$  band region of PHB/PLLA (75/25) blend during the isothermal crystallization process. Comparing the spectroscopic images based on the observation of the band position (Fig. S3a) with integrated absorbance of the crystalline PHB (Fig. S3b), the green region of the images in Fig. S3a corresponds to the yellow and red regions of image at 60 min in Fig. S3b. After 90 min, the blue region of the images in Fig. S3a corresponds to the red region of the images in Fig. S3b. The appearance of the blue region shown in the image

obtained based on the position of the spectral band indicates the disappearance of the intermolecular interaction between PHB and PLLA, which is consistent with the disappearance of the homogeneous region and the appearance of the red region shown in the image obtained based on the  $\nu(\text{C}=\text{O})$  absorbance. In the early stage of the isothermal crystallization process of the PHB-rich PHB/PLLA blend, the yellow and red region in the images based on the distribution of the integrated absorbance of  $\nu(\text{C}=\text{O})$  band of crystalline PHB correspond to the light blue and blue region based on the observation of the band position, respectively.

Compared with PHB/PLLA (50/50) blend,<sup>24</sup> the morphology of PHB/PLLA (75/25) blend after the isothermal crystallization process for 6 h is slightly different. A sea-island structure with crystalline PHB and crystalline PLLA can be observed, which is a three-dimensional continuous phase.

### Feasibility of Images Based on the Observation of the Band Position to Investigate the Isothermal Crystallization Process at Different Temperatures

In order to prove that the images obtained by distribution of the position of a spectral band are feasible to investigate the isothermal crystallization process at different temperatures, the isothermal crystallization process at  $140^\circ\text{C}$  was investigated. Figure 7 shows the images based on the observation of the band position and images based on the distribution of integrated absorbance of the  $\nu(\text{C}=\text{O})$  band of crystalline PHB ( $1730\text{--}1700\text{ cm}^{-1}$ ) of isothermal crystallization process in the PHB/PLLA (75/25) blend at  $140^\circ\text{C}$ . The disappearance of the intermolecular interaction between PHB and PLLA, which is indicated by fewer pixels with yellow and yellow green in corresponding images is based on the observation of the band position (Fig. 7a). The appearance of the inter- and intramolecular interactions within PHB crystal, which is indicated by more pixels with blue in the images based on the observation of the band position (Fig. 7a), was found to be constant with the

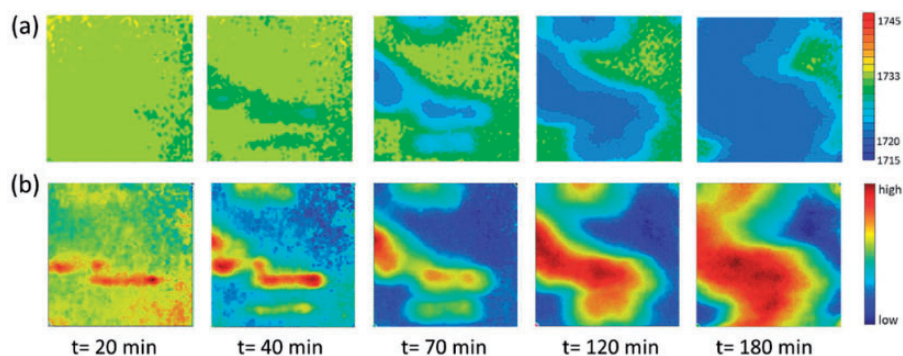


**Figure 7.** (a) ATR FT-IR images based on the peak position of the  $\nu(\text{C}=\text{O})$  band; (b) ATR FT-IR images generated by the distribution of integrated absorbance of the  $\nu(\text{C}=\text{O})$  band of PHB crystal ( $1730\text{--}1700\text{ cm}^{-1}$ ) during the isothermal crystallization at  $140^\circ\text{C}$  in the PHB/PLLA (75/25) blend as a function of time. The size of each image is  $0.6\text{ mm} \times 0.55\text{ mm}$ .

appearance of PHB crystal-rich domains in corresponding images based on the integrated  $\nu(\text{C}=\text{O})$  absorbance of PHB (Fig. 7b). It demonstrates that the peak images based on the observation of the band position and the images based on the integrated  $\nu(\text{C}=\text{O})$  absorbance of crystalline PHB show a good correspondence and can visualize the intra- and intermolecular interactions when investigating the isothermal crystallization process at different annealing temperatures.

## Conclusion

Physical and chemical properties of multicomponent polymer systems and their processing all depend on the inter- and intramolecular interactions occurring within them. The FT-IR spectroscopic images can reveal the distribution of component-rich domains in the imaged area, but they cannot show the areas where the intermolecular interactions occur. In order to highlight these areas, a novel technique based on the observation of the band position shift was introduced in this work. The peak shift of  $\nu(\text{C}=\text{O})$  band due to intermolecular interaction between PHB and PLLA in the FT-IR spectrum during the phase separation and crystallization process indicates the change of intra- and intermolecular interactions in the polymer blend. Thus, the images based on the observation of the band position were prepared in this study to visualize the distribution of different intra- and intermolecular interactions in PHB/PLLA blends during the isothermal crystallization process. The disappearance of the intermolecular interaction between PHB and PLLA, which is indicated in the images obtained based on the position of spectral band, agrees with the disappearance of homogeneous region shown in corresponding images based on the integrated absorbance of the  $\nu(\text{C}=\text{O})$  band. The appearance of the inter- and intramolecular interactions within PHB crystal, which is also indicated in the peak images based on the observation of the band position, agrees with the appearance of PHB crystal-rich domains in corresponding images based on the distribution of the integrated  $\nu(\text{C}=\text{O})$  absorbance of crystalline PHB. It is the first time the change of intra- and intermolecular interactions in the polymer blend has been visualized and the obtained images have been subsequently based on the observation of the band position. Compared to the images obtained by plotting the distribution of integrated absorbance of crystalline state of PHB, direct observation of specific intermolecular interactions based on band shift provides information about the strength of interactions that cannot be described by degree of crystallization. This work demonstrates that images based on the observation of the band position of spectral bands can reveal more information about the spatial distribution of different inter- and intramolecular interactions in the multicomponent polymer systems and their changes induced by

various perturbations, such as temperature, pressure, concentration, and pH.

## Declaration of Conflicting Interests

The author(s) declared no potential conflicts of interest with respect to the research, authorship, and/or publication of this article.

## Funding

The author(s) received no financial support for the research, authorship, and/or publication of this article.

## ORCID iD

Sergei G. Kazarian  <https://orcid.org/0000-0003-1768-9134>

## Supplemental Material

All supplemental material mentioned in the text, consisting of figures, is available in the online version of the journal.

## References

1. Y. Doi. *Microbial Polyesters*. New York, NY: VCH Publishers, 1990.
2. A.J. Anderson, E.A. Dawes. "Occurrence, Metabolism, Metabolic Role, and Industrial Uses of Bacterial Polyhydroxyalkanoates". *Microbiol. Rev.* 1990. 54(4): 450–472.
3. M. Vert. "Aliphatic Polyesters: Great Degradable Polymers That Cannot Do Everything". *Biomacromolecules*. 2005. 6(2): 538–546.
4. C. Bastioli. *Handbook of Biodegradable Polymers*. UK: Rapra Technology Limited, 2005.
5. C. Peña, T. Castillo, A. García, et al. "Biotechnological Strategies to Improve Production of Microbial Poly-(3-hydroxybutyrate): A Review of Recent Research Work". *Microb. Biotechnol.* 2014. 7(4): 278–293.
6. Y. Doi, A. Steinbüchel. *Biopolymers, Biology, Chemistry, Biotechnology, Applications, Volume 4, Polyesters III: Applications and Commercial Products*. Weinheim: Wiley-Blackwell, 2002.
7. R. Auras, L.-T. Lim, S.E.M. Selke, et al. *Poly(Lactic Acid): Synthesis, Structures, Properties, Processing, and Applications*. Hoboken, NJ: Wiley, 2010.
8. H. Tsuji. "Poly(Lactic Acid) Stereocomplexes: A Decade of Progress". *Adv. Drug Deliv. Rev.* 2016. 107(15): 97–135.
9. H. Urayama, T. Kanamori, Y. Kimura. "Properties and Biodegradability of Polymer Blends of Poly(L-lactide)S with Different Optical Purity of the Lactate Units". *Macromol. Mater. Eng.* 2002. 287(2): 116–121.
10. H. Sato, M. Nakamura, A. Padermshoke, et al. "Thermal Behavior and Molecular Interaction of Poly(3-hydroxybutyrate-Co-3-Hydroxyhexanoate) Studied by Wide-Angle X-ray Diffraction". *Macromolecules*. 2004. 37(10): 3763–3769.
11. H. Sato, R. Murakami, A. Padermshoke, et al. "Infrared Spectroscopy Studies of CH...O Hydrogen Bondings and Thermal Behavior of Biodegradable Poly(hydroxyalkanoate)". *Macromolecules*. 2004. 37(19): 7203–7213.
12. H. Sato, K. Mori, R. Murakami, et al. "Crystal and Lamella Structure and C-H...O=C Hydrogen Bonding of Poly(3-hydroxyalkanoate) Studied by X-ray Diffraction and Infrared Spectroscopy". *Macromolecules*. 2006. 39(4): 1525–1531.
13. H. Sato, Y. Ando, J. Dybal, et al. "Crystal Structures, Thermal Behaviors, and C-H...O=C Hydrogen Bondings of Poly(3-hydroxyvalerate) and Poly(3-hydroxybutyrate) Studied by Infrared Spectroscopy and X-ray Diffraction". *Macromolecules*. 2008. 41(12): 4305–4312.
14. L. Guo, H. Sato, T. Hashimoto, et al. "FTIR Study on Hydrogen-Bonding Interactions in Biodegradable Polymer Blends of

- Poly(3-hydroxybutyrate) and Poly(4-Vinylphenol)". *Macromolecules*. 2010. 43(8): 3897–3902.
15. L. Guo, H. Sato, T. Hashimoto, et al. "Thermally Induced Exchanges of Hydrogen Bonding Interactions and Their Effects on Phase Structures of Poly(3-hydroxybutyrate) and Poly(4-Vinylphenol) Blends". *Macromolecules*. 2011. 44(7): 2229–2239.
  16. N. Suttiwijitpukdee, H. Sato, J. Zhang, et al. "Effects of Intermolecular Hydrogen Bondings on Isothermal Crystallization Behavior of Polymer Blends of Cellulose Acetate Butyrate and Poly(3-hydroxybutyrate)". *Macromolecules*. 2011. 44(9): 3467–3477.
  17. I. Noda, M.M. Satkowski, A.E. Dowrey, et al. "Polymer Alloys of Nodax Copolymers and Poly(Lactic Acid)". *Macromol. Biosci*. 2004. 4(3): 269–275.
  18. M.A. Abdelwahab, A. Flynn, B.-S. Chiou, et al. "Thermal, Mechanical and Morphological Characterization of Plasticized PLA-PHB Blends". *Polym. Degrad. Stab*. 2012. 97(9): 1822–1828.
  19. I. Ohkoshi, H. Abe, Y. Doi. "Miscibility and Solid-State Structures for Blends of Poly(S)-Lactide with Atactic Poly(R,S)-3-hydroxybutyrate]. *Polymer*. 2000. 41(15): 5985–5992.
  20. J. Zhang, H. Sato, T. Furukawa, et al. "Crystallization Behaviors of Poly(3-hydroxybutyrate) and Poly(L-Lactic Acid) in Their Immiscible and Miscible Blends". *J. Phys. Chem. B*. 2006. 110(48): 24463–24471.
  21. E. Blümm, A.J. Owen. "Miscibility, Crystallization and Melting of Poly(3-hydroxybutyrate)/Poly(L-Lactide) Blends". *Polymer*. 1995. 36(21): 4077–4081.
  22. N. Koyama, Y. Doi. "Miscibility of Binary Blends of Poly(R)-3-hydroxybutyric Acid, and Poly(S)-Lactic Acid]. *Polymer*. 1997. 38(7): 1589–1593.
  23. C. Vogel, E. Wessel, H.W. Siesler. "FT-IR Imaging Spectroscopy of Phase Separation in Blends of Poly(3-hydroxybutyrate) with Poly(L-lactic Acid) and Poly( $\epsilon$ -caprolactone)". *Biomacromolecules*. 2008. 9(2): 523–527.
  24. H. Lu, S.G. Kazarian, H. Sato. "Simultaneous Visualization of Phase Separation and Crystallization in PHB/PLLA Blends with In Situ ATR-FTIR Spectroscopic Imaging". *Macromolecules*. 2020. 53(20): 9074–9085.
  25. K.L.A. Chan, S.G. Kazarian, D. Vassou, et al. "In Situ High-Throughput Study of Drug Polymorphism Under Controlled Temperature and Humidity Using FT-IR Spectroscopic Imaging". *Vib. Spectrosc*. 2007. 43(1): 221–226.
  26. H. Shinzawa, K. Awa, Y. Ozaki, et al. "Near-Infrared Imaging Analysis of Cellulose Tablet by a Band Position Shift". *Appl. Spectrosc*. 2009. 63(8): 974–977.
  27. H. Shinzawa, K. Awa, Y. Ozaki. "Compression-Induced Morphological and Molecular Structural Changes in Cellulose Tablets Probed by Near-Infrared Imaging". *J. Near Infrared Spectrosc*. 2011. 19(1): 15–22.
  28. Q. Guo. "Polymer Morphology: Principles, Characterization, and Processing". Hoboken, NJ: John Wiley and Sons, 2016.
  29. A.V. Ewing, S.G. Kazarian. "Infrared Spectroscopy and Spectroscopic Imaging in Forensic Science". *Analyst*. 2017. 142(2): 257–272.
  30. H. Lu, H. Shinzawa, S.G. Kazarian. "Intermolecular Interactions in the Polymer Blends Under High-Pressure CO<sub>2</sub> Studied Using Two-Dimensional Correlation Analysis and Two-Dimensional Disrelation Mapping". *Appl. Spectrosc*. 2021. 75(3): 250–258.
  31. H. Lu, S.G. Kazarian. "How Does High-Pressure CO<sub>2</sub> Affect the Morphology of PCL/PLA Blends? Visualization of Phase Separation Using In Situ ATR-FTIR Spectroscopic Imaging". *Spectrochim. Acta, Part. A*. 2020. 243: 118760.
  32. C.L. Song, S.G. Kazarian. "Effect of Controlled Humidity and Tissue Hydration on Colon Cancer Diagnostic via FTIR Spectroscopic Imaging". *Anal. Chem*. 2020. 92(14): 9691–9698.
  33. K.L.A. Chan, A. Altharawi, F. Fale, et al. "Transmission Fourier Transform Infrared Spectroscopic Imaging, Mapping, and Synchrotron Scanning Microscopy with Zinc Sulfide Hemispheres on Living Mammalian Cells at Sub-Cellular Resolution". *Appl. Spectrosc*. 2020. 74(5): 544–552.
  34. P. Lasch, I. Noda. "Two-Dimensional Correlation Spectroscopy (2D-COS) for Analysis of Spatially Resolved Vibrational Spectra". *Appl. Spectrosc*. 2019. 73(4): 359–379.
  35. Y. Hikima, J. Morikawa, S.G. Kazarian. "Analysis of Molecular Orientation in Polymeric Spherulite Using Polarized Micro Attenuated Total Reflection Fourier Transform Infrared (ATR-FTIR) Spectroscopic Imaging". *Anal. Chim. Acta*. 2019. 1065: 79–89.
  36. T. Furukawa, H. Sato, R. Murakami, et al. "Structure, Dispersibility, and Crystallinity of Poly(Hydroxybutyrate)/Poly(L-Lactic Acid) Blends Studied by FT-IR Microspectroscopy and Differential Scanning Calorimetry". *Macromolecules*. 2005. 38(15): 6445–6454.